Carboxylate substitution position influencing polymer properties and enabling non-fullerene organic solar cells with high open circuit voltage and low voltage loss

Jing Liu[1,2]†, Lik-Kuen Ma[2]†, Fu Kit Sheong[2], Lin Zhang[3], Huawei Hu[4], Jing-Xuan Zhang[2], Jianquan Zhang[2], Zhengke Li[5], Chao Ma[6], Xu Han[6], Ding Pan[7], Harald Ade[4], Wei Ma[3], and He Yan[1,2]*

[1] The Hong Kong University of Science and Technology-Shenzhen Research Institute No. 9 Yuexing 1st RD, Hi-tech Park, Nanshan Shenzhen 518057, China
*Email: hyan@ust.hk

[2] Department of Chemistry and Hong Kong Branch of Chinese National Engineering Research Center for Tissue Restoration & Reconstruction, Hong Kong University of Science and Technology, Clear Water Bay, Kowloon, Hong Kong

[3] State Key Laboratory for Mechanical Behavior of Materials, Xi'an Jiaotong University, Xi'an 710049, China

[4] Department of Physics, North Carolina State University, Raleigh, North Carolina 27695, United States

[5] School of Material Science and Engineering, Sun Yat-Sen University, No. 135 West Xingang RD, Guangzhou 510275, China

[6] Department of Physics, Hong Kong University of Science and Technology, Clear Water Bay, Kowloon, Hong Kong

[7] Department of Physics and Department of Chemistry, Hong Kong University of Science and Technology, Clear Water Bay, Kowloon, Hong Kong; HKUST Fok Ying Tung Research Institute, Guangzhou, China

†These authors contributed equally to this work.

Abstract

To minimize the voltage loss of non-fullerene organic solar cells (OSCs), it is important to modulate the energy levels of active materials and thus the photovoltage of the device. In this paper, we report a simple and effective approach to tune the energy levels of a state-of-art polymer P3TEA by switching the position of alkyl side chains and carboxylate substituents on the polymer backbone. The resulting polymer P3TAE exhibits a deep highest occupied molecular orbital (HOMO) level, contributing to a high open circuit voltage (V_{OC}) of 1.20 V and a small voltage loss of 0.54 V when it is blended with a small molecule acceptor (SMA) FTTB-PDI4. Despite a small charge separation driving force, the P3TAE:FTTB-PDI4 blend

exhibits efficient charge extraction, supported by relatively high external quantum efficiency (EQE) (~60%) in the according device. In addition, the P3TAE:FTTB-PDI4 blend shows relatively high electron mobility and domain purity, leading to a high fill factor (FF) in the device. As a result, the P3TAE:FTTB-PDI4-based solar cell exhibits a power conversion efficiency (PCE) of 8.10%, which is one of the highest achieved performances for single-junction OSCs with V_{OC} higher than 1.20 V.

Introduction

Bulk heterojunction (BHJ) OSCs have attracted considerable academic and industrial interest in the past three decades due to their promising advantages, such as low cost, light weight and mechanically flexibility.[1-7] For a high performing OSC, it should contain an active layer with the following features, strong absorption over a broad solar spectrum, suitable molecular energy level alignment, and favorable nanoscale morphology for efficient charge generation and transportation.[8-10] Consequently, highly efficient OSCs are achievable upon the optimization of three key parameters, EQE, V_{OC} and FF. For fullerene-based OSCs, the increase of OSC performance is mainly driven by the rational design of donor polymers, which leads to the best efficiency of 11.7%.[4] However, the performance of this state-of-art fullerene OSC is limited by the relatively large voltage loss defined as the difference between the optical bandgap of the donor polymer (1.65 eV) and the V_{OC} in this cell (0.78 V). Further improvement towards more efficient fullerene OSCs is challenging unless the OSC community could reduce the voltage loss without sacrificing the short circuit current (J_{SC}) and FF.[11-14]

In contrast to fullerene acceptors, non-fullerene acceptors have emerged as promising alternatives due to their prevailing advantages of easy accessibility, strong absorption in both visible and NIR region, and better tunable functionality.[15-32] More importantly, it appears that the non-fullerene systems can still work efficiently even with a negligible charge separation driving force.[33-35] Therefore, the large voltage losses in fullerene OSC systems could be significantly reduced in non-fullerene OSCs, which is beneficial for achieving larger V_{OC} and thus better device performance.

In order to improve the V_{OC} of the BHJ blend, the energy level alignment between the donor and acceptor materials must be fine-tuned.[36-38] Over the past few decades, many research efforts have been devoted to improve the V_{OC} of OSCs by rationally down-shifting the HOMO level of donor polymers. For example, carboxylate substitution was employed by Hou and coworkers to modify P3HT, resulting in a significant enhancement of V_{OC} (from 0.63 V to 0.91 V) and device performance.[39] It is also worth mentioning that one of the state-of-art work reported a novel donor polymer P3TEA with a low-lying HOMO level of -5.37 eV.[33] When P3TEA was combined with a reported SMA named SF-PDI$_2$, the solar cell achieved a PCE of 9.5% with a high V_{OC} of 1.11 V despite a negligible driving force for charge separation. Consequently, the voltage loss in this system is estimated to be 0.58 V considering the optical bandgap of P3TEA is 1.69 eV. This work demonstrates the first example of efficient charge separation despite a small driving force. The key factor of design rationale in this system is the employment of the carboxylate substitution on the polymer backbone, which is a promising and effective approach to tune the V_{OC} of non-fullerene OSCs.

Herein, we attempt to further push the energy level limit of P3TEA to obtain a higher V_{OC} via rational modification. By exchanging the position of alkyl side chains and carboxylate substituents on the backbone of P3TEA, we obtain a novel analog polymer P3TAE. The major difference between P3TAE and P3TEA is the position of the carboxylate substitution, which is found to influence the electrical and optical properties, hole mobility, and aggregation tendence of donor polymers significantly. For P3TAE, the HOMO level is effectively down-shifted by ~0.18 eV while the LUMO level is slightly up-shifted compared to P3TEA, which is in good agreement with the calculated results. Therefore, P3TAE exhibits a blue-shifted absorption and larger optical bandgap (1.74 eV). In addition, theoretical calculation demonstrates a more twisted backbone for P3TAE evidenced by the overall smaller dihedral angles in each polymer repeating unit, leading to weaker molecular packing and crystallinity of P3TAE than P3TEA, which is further supported by hole mobility and morphology data of two neat polymer films. When P3TAE is combined with the SMA SF-PDI$_2$, the device exhibits a PCE of 7.12% with a high V_{OC} of 1.19 V, a J_{SC} of 10.98 mA cm^{-2}, and a FF of 0.55. Higher efficiency of the cell is realized when P3TAE is combined with

another PDI-based SMA FTTB-PDI4. To our surprise, P3TAE:FTTB-PDI4-based solar cell achieves an enhanced PCE of 8.10% with a higher V_{OC} of 1.20 V and an elevated FF of 0.65, indicating the voltage loss of this system is effectively reduced to 0.54 V. Importantly, the 8.10% performance is one of the highest achieved values for non-fullerene OSCs with V_{OC} larger than 1.20 V. Further study of morphological characterizations shows that the main reasons for elevated FF and PCE of the P3TAE:FTTB-PDI4 blend are the higher electron mobility and domain purity than the P3TAE:SF-PDI$_2$ blend. To conclude, the small modification of the polymer backbone brings significant differences in molecular properties and device performance, demonstrating our simple and effective design strategy is promising to push the limit of polymer energy levels to achieve efficient non-fullerene OSCs with higher V_{OC} and lower voltage loss.

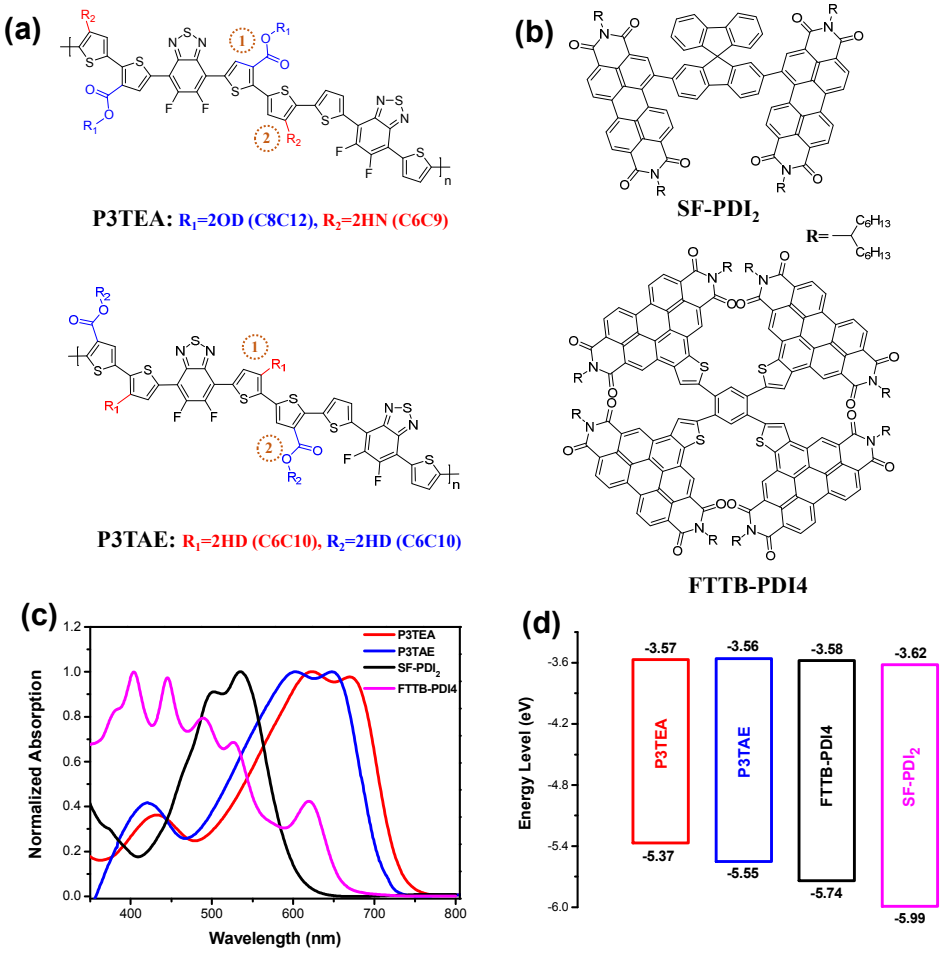

Fig. 1 (a) Chemical structures of P3TEA and P3TAE polymers. The first thiophene and the second thiophene on P3TEA and P3TAE are labelled for better comparison. (b) Chemical structures of two small

molecule acceptors SF-PDI$_2$ and FTTB-PDI4. (c) Normalized UV-vis absorption spectra and (d) energy levels of two polymers and two small molecules.

Results and discussion

Fig. 1a is the chemical structures of two analog polymers P3TEA and P3TAE, which exhibit similar molecular backbone except the position of the alkyl side chains and the carboxylate substituents. With the alkyl chain on the first thiophene and the carboxylate substituent on the second thiophene (as labelled in Fig. 1a), P3TAE was successfully synthesized according to the synthetic route of P3TEA.[33] The length of alkyl chains situated on the first thiophene and the carboxylate substituent (R_1 and R_2) of P3TAE is further optimized to match the non-fullerene acceptors. After several attempts, when both R_1 and R_2 are 2-hexyldecyl (2HD) alkyl chains, polymer-based solar cells can achieve the highest performance. High-temperature gel permeation chromatograpy (GPC) was employed to measure the number-average and weight-average molecular weight (M_n and M_w) of P3TAE, which are 94.2 kDa and 214.6 kDa, respectively, demonstrating a polydispersity index (PDI) of 2.28 for P3TAE.

The UV-vis absorption spectra of P3TEA, P3TAE, SF-PDI$_2$ and FTTB-PDI4 thin films are shown in Fig. 1c, in which P3TAE exhibits a ~20 nm blue-shifted absorption than P3TEA. The film absorption onset of P3TAE and P3TEA as determined in Fig. S1a are 713 nm and 733 nm, indicating an optical bandgap of 1.74 eV for P3TAE and 1.69 eV for P3TEA.[11, 14, 40] The polymer donor and the SMA exhibit complementary absorption over the range of 400-700 nm, which is expected to efficiently convert the solar energy to electricity in this region (Fig. 1c). The self-aggregation properties of P3TEA and P3TAE are evidenced by temperature-dependent UV-vis absorption as shown in Fig.S2. During the cooling process of polymer solutions from 100 ^{o}C to 20 ^{o}C, the absorption spectra are gradually red-shifted, indicating certain aggregation of two polymers. When the temperature of the polymer solution is cooled to room temperature, there is a small peak shoulder appeared at around 690 nm for P3TEA and at 680 nm for P3TAE, indicating π-π intermolecular interaction of two polymers. To clearly illustrate the extent of polymer aggregation of two polymers, we induce the parameter “relative aggregation strength”,[41, 42] which is defined as the normalized intensity of

each peak (at 631 nm for P3TEA and 608 nm for P3TAE) to the intensity of the maximum absorption at 20 ^{o}C. After extracting the data of absorption spectra in Fig. S2a and S2b, the "relative aggregation strength" was plotted versus the solution temperature in Fig. S2c. The aggregation property of two polymers are similar during the cooling process, yet it could be clearly observed that P3TEA exhibits stronger tendency of aggregation than P3TAE. P3TEA and P3TAE show similar chemical structures except the position of carboxylate substitutions along the polymer backbone, yet P3TAE exhibits blue-shifted absorption and lower propensity of aggregation compared to P3TEA.

Cyclic voltammetry (CV) measurement (Fig. S3) was employed to get the energy levels of P3TAE. The HOMO and LUMO levels for P3TAE were estimated to be -5.55 and -3.56 eV from the onset of oxidation and reduction potentials. The energy levels of P3TEA, SF-PDI$_2$ and FTTB-PDI4 are directly extracted from our previous paper, which were collected by the same experimental method.[33, 34] It is interesting to notice that P3TAE exhibits similar LUMO level to P3TEA, while the HOMO level of P3TAE was decreased by 0.18 eV compared to P3TEA, which is beneficial for achieving high V_{OC} and low voltage loss in OSCs. Notably, the LUMO-LUMO energy offset between P3TAE and two SMAs is within 0.10 eV, which is relatively small compared to general OSC systems.

In order to further demonstrate the difference of optical and electrical properties between P3TEA and P3TAE, theoretical calculations of two polymers were conducted by DFT method at a level of B3LYP/6-31G*. For simplification, all the alkyl chains were replaced with methyl groups and the according energy distributions of P3TEA and P3TAE are shown in Fig.S4. From the calculation results, LUMO levels of P3TEA and P3TAE are -2.96 and -2.91 eV, respectively. However, P3TAE exhibits a deeper HOMO level of -5.15 eV than P3TEA (-5.08 eV). Overall, P3TAE exhibits a shallower LUMO level but a deeper HOMO level than P3TEA, which is in good agreement with the aforementioned CV measurements. One possible explanation is that for P3TAE, the electron-withdrawing thiophene-carboxylate unit is surrounded by two neighboring thiophenes, which are the donor part of P3TAE. It can be interpreted that the electron-withdrawing carboxylate substitution has a major influence on

the donor unit of P3TAE, leading to distinct decrease of the HOMO level. However, for P3TEA, there are both donor unit (thiophene) and acceptor unit (difluorobenzothiadiazole, ffBT) on two sides of the thiophene-carboxylate, hence the electron-withdrawing carboxylate substitution relatively has a weaker effect on the donor part and a stronger effect on the acceptor part compared to P3TAE. Therefore, P3TEA exhibits a shallower HOMO level than P3TAE. Importantly, the electron-withdrawing ability of thiophene-carboxylate unit is much weaker than ffBT, suggesting the LUMO level of P3TEA is mainly determined by ffBT and the thiophene-carboxylate unit induce limited decrease of the LUMO level of P3TEA. To conclude, P3TEA shows an up-shifted HOMO level but a slightly down-shifted LUMO level than P3TAE, leading to the shrunken optical bandgap for P3TEA.

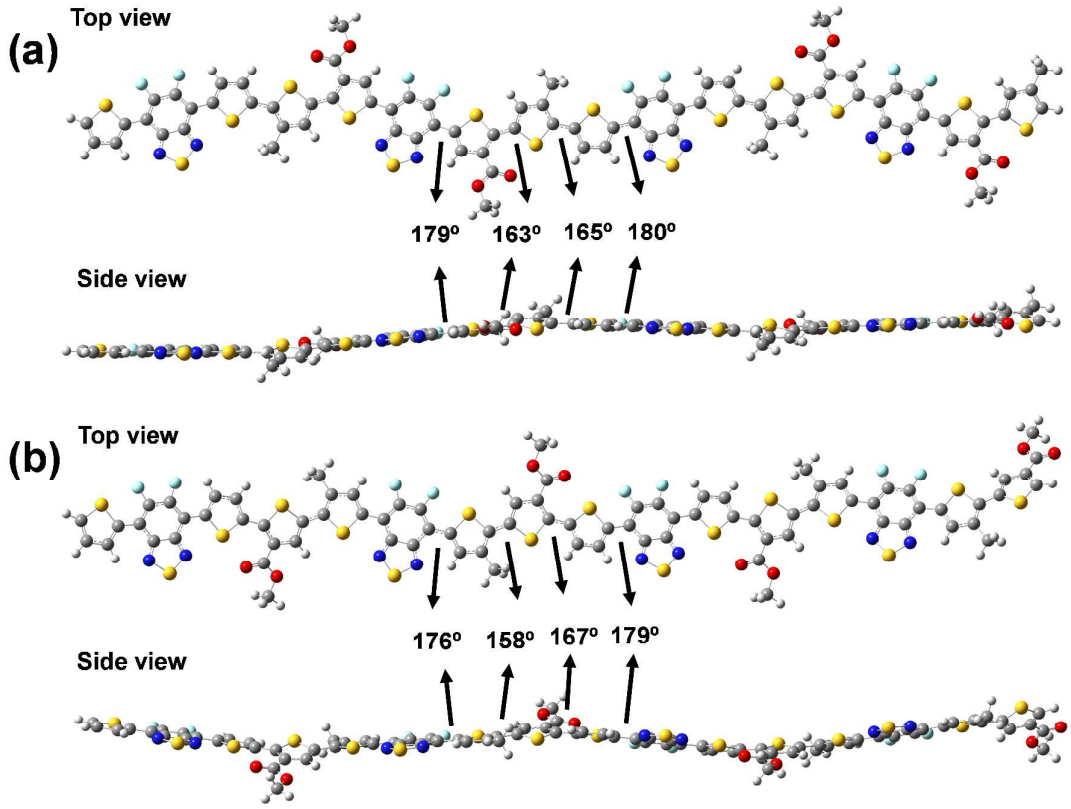

Fig.2 Top and side views of the optimized conformations of (a) P3TEA, and (b) P3TAE dimers based on the calculation results.

The optimal structural conformations of two polymer dimers were also calculated and shown in Fig.2 with their respective dihedral angles between two adjacent ffBT units listed. For P3TEA, the C-C-C-S, C-C-C-C, S-C-C-S and C-C-C-C dihedral angles between two adjacent

ffBT units are 179º, 163º, 165º and 180º, respectively, which are 176º, 158º, 167º and 179º for P3TAE, demonstrating a more twisted molecular backbone for P3TAE. For a good polymer donor in the non-fullerene OSC system, it should keep reasonable solubility in common solvents for the device processing while simultaneously maintain certain molecular crystallinity to guarantee a favorable blend morphology. As the backbone of P3TAE is more twisted, the length of R_1 and R_2 should be slightly shorter than those of P3TEA to achieve a better balance between polymer solubility and crystallinity. After several trial and error, 2-hexyldecyl and 2-hexyldecyl alkyl chains are proven to be the optimal choice for R_1 and R_2 to achieve the best performing OSCs.

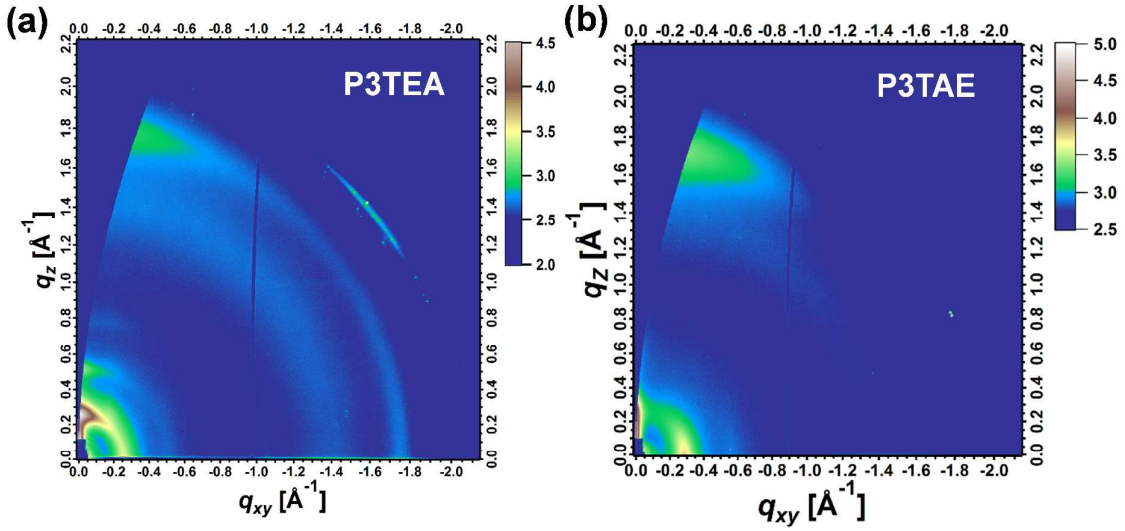

Fig. 3 2D GIWAXS patterns of (a) P3TEA, (b) P3TAE films.

To gain more insights into the difference of molecular packing and crystallinity between P3TEA and P3TAE, grazing-incidence wide-angle X-ray scattering (GIWAXS) was implemented on two polymer neat films. From the 2D GIWAXS patterns in Fig. 3, P3TEA exhibits a higher order of lamellar stacking and even (300) stacking peak is slightly visible in the out-of-plane direction. The π-π stacking distance of P3TAE and P3TEA are 3.65 Å and 3.57 Å, respectively, indicating closer molecular packing of P3TEA. Also, P3TAE exhibits a shorter (010) coherence length of 30 Å than that of P3TEA (38 Å). The above GIWAXS data demonstrates weaker aggregation of P3TAE than P3TEA, which is mainly attributed to more twisted molecular backbone of P3TAE. To further verify this, the space-charge-limited current

(SCLC) method was employed to measure the charge mobility of two donor polymers (Fig. S5a). The hole mobility for P3TAE neat film is calculated to be 6.04×10^{-4} cm^2 V^{-1} s^{-1}, which is lower than P3TEA (7.72×10^{-4} cm^2 V^{-1} s^{-1}), showing good accordance with the above GIWAXS data.

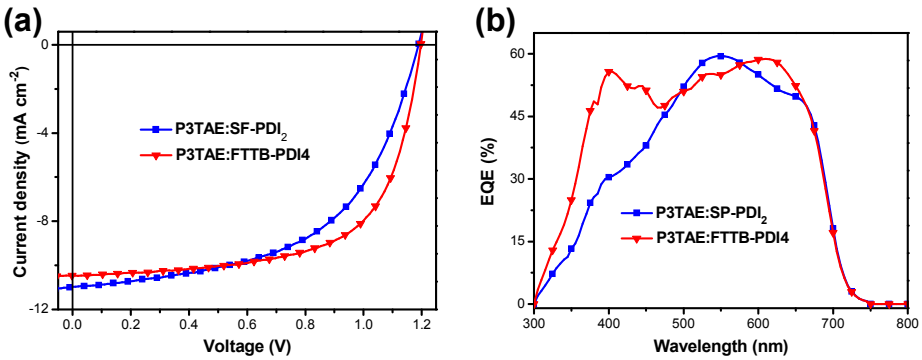

Fig.4 (a) *J-V* and (b) EQE curves of solar cells based on P3TAE:SF-PDI_2 and P3TAE:FTTB-PDI4 blends.

To investigate the device performance of non-fullerene OSCs based on the newly designed polymer P3TAE, an inverted structure of glass/indium tin oxide (ITO)/ZnO/active layer/V_2O_5/Al was fabricated. The details of the device fabrication are shown in the supporting information. When P3TAE is blended with a reported SMA SF-PDI_2, upon the optimization of the D/A weight ratio and the processing condition, the most efficient device shows a PCE of 7.12%, with a high V_{OC} of 1.19 V, a J_{SC} of 10.98 mA cm^{-2} and a FF of 0.55 (Table 1). Further optimization of device performance was realized when P3TAE was combined with another SMA named FTTB-PDI4.[34] The P3TAE:FTTB-PDI4-based device exhibits a high V_{OC} of 1.20 V, a J_{SC} of 10.47 mA cm^{-2}, a FF of 0.65, leading to an elevated performance of 8.10% (Table 1), which is one of the highest achieved values of single-junction OSCs with $\geqslant$1.20 V V_{OC} to date. Considering the optical bandgap of P3TAE is 1.74 eV, the voltage loss in our system is effectively reduced to 0.54 V. For consistent comparison of our work with other systems with low voltage losses, we measured the bandgap of P3TAE based on fitting equations of absorption and emission originating from Marcus theory.[33, 43] In this way, the bandgap of P3TAE is determined to be 1.81 eV as the crossing point of normalized polymer absorption and emission curves (Fig. S1b), which demonstrates a voltage loss of 0.61 V for our P3TAE:FTTB-PDI4-based blend. In addition,

even though the driving force in the P3TEA:SF-PDI_2 and P3TAE:FTTB-PDI4 blends is nearly zero, the charge generation of our systems is still efficient evidenced by considerable response of EQE spectra over the region of 300-700 nm. In particular, the high EQE value (up to ~60% for P3TEA:SF-PDI_2 and P3TAE:FTTB-PDI4) of two devices in the 550-700 nm region, which belongs to absorption range of P3TAE, indicates photons absorbed by P3TAE are efficiently converted to electrons despite the negligible driving force. The current density integrated from the EQE spectrum was 10.46 mA cm^{-2} for the P3TAE:FTTB-PDI4-based device, validating the accuracy of our device measurement.

Table 1 Photovoltaic parameters of solar cells based on P3TAE:SF-PDI_2 and P3TAE:FTTB-PDI4 blends.

Active materials	V_{OC} [V]	J_{SC} [mA cm^{-2}]	FF [%]	PCE [%]	Average PCE[a)] [%]
P3TAE:SF-PDI_2	1.19	10.98	0.55	7.12	6.81±0.16
P3TAE:FTTB-PDI4	1.20	10.47	0.65	8.10	7.83±0.20

a) The average values of PCE for over 7 devices.

The OSC performance of our P3TAE:FTTB-PDI4 device was also compared with the reported P3TEA:FTTB-PDI4-based system as shown in Fig. S6a. The P3TEA:FTTB-PDI4-based cell exhibits a lower V_{OC} of 1.13 V, a similar FF of 0.66, yet a higher J_{SC} of 13.96 mA cm^{-2} compared to the P3TAE:FTTB-PDI4 system, leading to its generally higher solar cell efficiency of 10.33%. The higher current and performance of P3TEA:FTTB-PDI4-based device may be ascribed to the red-shifted absorption of P3TEA and thus relatively stronger photon harvesting ability of the cell in the long-wavelength region. As the optical bandgap of P3TEA is 1.69 eV, the P3TEA:FTTB-PDI4-based cell presents a larger voltage loss of 0.56 V. As a result, though our P3TAE:FTTB-PDI4 device exhibits a lower performance than P3TEA:FTTB-PDI4-based cell, it realizes both higher V_{OC} and lower voltage loss through simple but efficient modification of donor polymer structure, which opens up many possibilities to pursue low voltage loss for efficient OSCs at the material synthesis level.

Compared with P3TAE:SF-PDI_2-based device, the prevailing device parameter of P3TAE:FTTB-PDI4-based one is the enhanced FF, which could be explained by the relatively higher electron mobility of FTTB-PDI4 than SF-PDI_2 in the blend. SCLC measurements

show that the electron mobilities of P3TAE:SF-PDI$_2$ and P3TAE:FTTB-PDI4 blends are calculated to be 1.43×10^{-4} and 5.52×10^{-4} cm^2 V^{-1} s^{-1}, and the hole mobilities of two blends are 5.37×10^{-4} and 5.33×10^{-4} cm^2 V^{-1} s^{-1}, respectively (Fig. S5b, c). The four times higher electron mobility and balanced hole/electron mobility in the P3TAE:FTTB-PDI4 blend contribute to efficient charge transportation and collection in the vertical direction of the device and thus higher FF and PCE of the device.

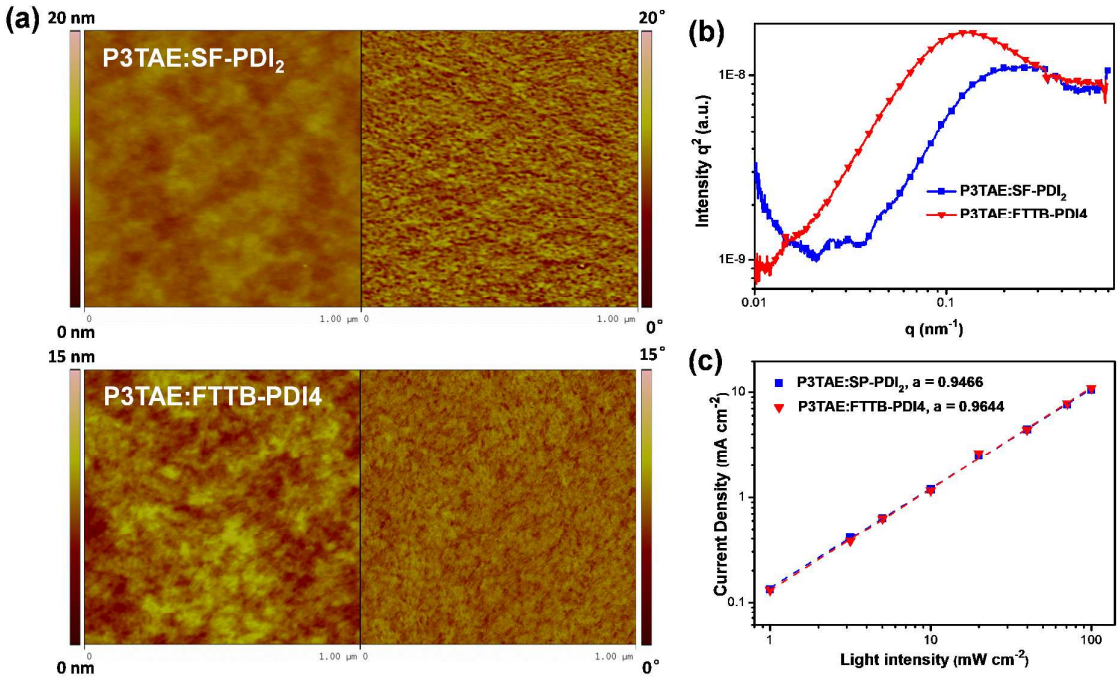

Fig. 5 (a) AFM hight (left) and phase (right) images, (b) R-SoXS profiles, and (c) the current versus the light intensity of P3TAE:SF-PDI$_2$ and P3TAE:FTTB-PDI4 blends. Dashed lines are linear fitting results.

The 2D GIWAXS patterns of P3TAE:SF-PDI$_2$ and P3TAE:FTTB-PDI4 blends were also characterized as shown in Fig. S7, which demonstrated similar ordering of donor polymer and small molecules in two blend films. To achieve more insights of performance difference of two systems, atomic force microscopy (AFM) and resonant soft X-ray scattering (R-SoXS) were conducted to investigate their device morphology. The height and phase images of two blends are shown in Fig. 5a, demonstrating quite uniform and smooth surface without clear phase separation. The R-SoXS profiles of P3TAE:SF-PDI$_2$ and P3TAE:FTTB-PDI4 blends are depicted in Fig.5b to provide quantitative morphological information. It can be observed

that there is a peak at 0.236 nm^{-1} for the P3TAE:SF-PDI_2 device, indicating a small domain size of 13.2 nm assuming a two-phase morphology, whereas P3TAE:FTTB-PDI4 exhibits a comparatively larger domain size of 23.5 nm. However, P3TAE:FTTB-PDI4 was found to exhibit a much higher domain purity than P3TAE:SF-PDI_2 (1 vs 0.89), which is in good agreement with the aforementioned higher electron mobility of the P3TAE:FTTB-PDI4 blend. Though P3TAE:FTTB-PDI4 exhibits larger domain sizes that may lead to slightly decreased J_{SC} of the device, the enhanced domain purity contributes to the remarkable elevation of FF from 0.55 to 0.65, which brings an overall enhanced PCE for P3TAE:FTTB-PDI4-based solar cells.

Lastly, the dependence of J_{SC} on the light intensity was measured to reveal the bimolecular recombination behavior in the P3TAE:SF-PDI_2 and P3TAE:FTTB-PDI4 blends (Fig. 5c). The relationship between J_{SC} and the light intensity can be expressed as $J_{SC} \propto P^{\alpha}$, where P is the light intensity and α is the recombination index. In ideal conditions, if all the free charges can be collected by two electrodes before recombination, α should equal to 1. However, some degree of bimolecular recombination in the OSC systems should lead to the <1 value of α, and the more severe the bimolecular recombination is, the lower α value would be.[44] As revealed in Fig. 5b, the calculated α values for P3TAE:SF-PDI_2 and P3TAE:FTTB-PDI4 blends are 0.9466 and 0.9644, respectively. Therefore, the P3TAE:FTTB-PDI4 blend exhibits more suppressed bimolecular recombination than P3TAE:SF-PDI_2, which may be ascribed to the relatively higher domain purity of the P3TAE:FTTB-PDI4 blend. This provides another explanation for the better performance of P3TAE:FTTB-PDI4-based OSCs.

Conclusions

In conclusion, we synthesized a new terthiophene-based polymer P3TAE via the exchange of the position of carboxylate substituents and the alkyl side chains on the backbone of a reported polymer P3TEA. Compared with P3TEA, the obtained polymer P3TAE shows ~0.18 eV down-shifted HOMO level, ~20 nm blue-shifted absorption and a larger optical bandgap of 1.74 eV. Besides, P3TAE exhibits a more twisted molecular backbone than P3TEA, leading to weaker molecular aggregation and crystallinity of P3TAE. Our simple and effective design

strategy demonstrates its great potential to effectively tune the properties of donor polymers. When P3TAE is combined with two SMA SF-PDI_2 and FTTB-PDI4, P3TAE:FTTB-PDI4 can obtain a higher PCE of 8.10% than the P3TAE:SF-PDI_2-based blend (7.12%). Besides, P3TAE:FTTB-PDI4-based devices can achieve a V_{OC} of up to 1.20 V, indicating a small voltage loss of 0.54 V. To the best of our knowledge, the PCE of 8.10% is one of the highest achieved values in the single-junction OSCs with a high V_{OC} of ≥1.20 V. Importantly, the driving force between the polymer and SMA is negligible, yet it does not cause any negative effect on the charge generation and transportation. These results demonstrate our novel polymer is promising to achieve efficient non-fullerene OSCs with high V_{OC} and low voltage loss.

Conflicts of interest

The authors declare no conflicts of interest.

Acknowledgements

The work described in this paper was partially supported by the National Basic Research Program of China (973 Program project numbers 2013CB834701 and 2014CB643501), the ShenZhen Technology and Innovation Commission (project number JCYJ20170413173814007), the Hong Kong Research Grants Council (project numbers T23–407/13 N, N_HKUST623/13, 16305915, 16322416, 606012, and 16303917), HK JEBN Limited, HKUST president's office (Project FP201), the National Science Foundation of China (#21374090), the Ministry of Science and Technology of China (No. 2016YFA0200700), and NSFC (21504066). X-ray data were acquired at Advanced Light Source, which was supported by the Director, Office of Science, Office of Basic Energy Sciences, of the U.S. Department of Energy under Contract No. DE-AC02-05CH11231.

References

[1] G. Yu, J. Gao, J. C. Hummelen, F. Wudl, A. J. Heeger, *Science*, 1995, **270**, 1789-1791.
[2] G. Li, V. Shrotriya, J. Huang, Y. Yao, T. Moriarty, K. Emery, Y. Yang, *Nat. Mater.*, 2005,

4, 864-868.
[3] Y. Liu, J. Zhao, Z. Li, C. Mu, W. Ma, H. Hu, K. Jiang, H. Lin, H. Ade, H. Yan, *Nat. Commun.*, 2014, **5**, 5293.
[4] J. Zhao, Y. Li, G. Yang, K. Jiang, H. Lin, H. Ade, W. Ma, H. Yan, *Nat. Energy*, 2016, **1**, 15027.
[5] A. J. Heeger, *Adv. Mater.*, 2014, **26**, 10-27.
[6] Z. He, B. Xiao, F. Liu, H. Wu, Y. Yang, S. Xiao, C. Wang, T. P. Russell, Y. Cao, *Nat. Photon.*, 2015, **9**, 174-179.
[7] Z. He, C. Zhong, S. Su, M. Xu, H. Wu, Y. Cao, *Nat. Photon.*, 2012, **6**, 591-595.
[8] H. Yao, L. Ye, H. Zhang, S. Li, S. Zhang, J. Hou, *Chem. Rev.*, 2016, **116**, 7397-7457.
[9] J. Zhao, Y. Li, A. Hunt, J. Zhang, H. Yao, Z. Li, J. Zhang, F. Huang, H. Ade, H. Yan, *Adv. Mater.*, 2016, **28**, 1868-1873.
[10] W. Zhao, S. Li, H. Yao, S. Zhang, Y. Zhang, B. Yang, J. Hou, *J. Am. Chem. Soc.*, 2017, **139**, 7148-7151.
[11] W. Li, K. H. Hendriks, A. Furlan, M. M. Wienk, R. A. Janssen, *J. Am. Chem. Soc.*, 2015, **137**, 2231-2234.
[12] K. Vandewal, Z. Ma, J. Bergqvist, Z. Tang, E. Wang, P. Henriksson, K. Tvingstedt, M. R. Andersson, F. Zhang, O. Inganäs, *Adv. Func. Mater.*, 2012, **22**, 3480-3490.
[13] M. Wang, H. Wang, T. Yokoyama, X. Liu, Y. Huang, Y. Zhang, T. Q. Nguyen, S. Aramaki, G. C. Bazan, *J. Am. Chem. Soc.*, 2014, **136**, 12576-12579.
[14] K. Kawashima, Y. Tamai, H. Ohkita, I. Osaka, K. Takimiya, *Nat. Common.*, 2015, **6**, 10085.
[15] Y. Lin, J. Wang, Z.-G. Zhang, H. Bai, Y. Li, D. Zhu, X. Zhan, *Adv. Mater.*, 2015, **27**, 1170-1174.
[16] Y. Lin, Z.-G. Zhang, H. Bai, J. Wang, Y. Yao, Y. Li, D. Zhu, X. Zhan, *Energy Environ. Sci.*, 2015, **8**, 610-616.
[17] S. Li, L. Ye, W. Zhao, S. Zhang, S. Mukherjee, H. Ade, J. Hou, *Adv. Mater.*, 2016, **28**, 9423-9429.
[18] H. Yao, Y. Chen, Y. Qin, R. Yu, Y. Cui, B. Yang, S. Li, K. Zhang, J. Hou, *Adv. Mater.*, 2016, **28**, 8283-8287.
[19] Y. Cui, C. Yang, H. Yao, J. Zhu, Y. Wang, G. Jia, F. Gao, J. Hou, *Adv. Mater.*, 2017, **29**, 1703080.
[20] S. Li, L. Ye, W. Zhao, X. Liu, J. Zhu, H. Ade, J. Hou, *Adv. Mater.*, 2017, **29**, 1704051.
[21] H. Yao, L. Ye, J. Hou, B. Jang, G. Han, Y. Cui, G. M. Su, C. Wang, B. Gao, R. Yu, H. Zhang, Y. Yi, H. Y. Woo, H. Ade, J. Hou, *Adv. Mater.*, 2017, **29**, 1700254.
[22] J. Zhu, Z. Ke, Q. Zhang, J. Wang, S. Dai, Y. Wu, Y. Xu, Y. Lin, W. Ma, W. You, X. Zhan, *Adv. Mater.*, 2017, **30**, 1704713.
[23] B. Jia, S. Dai, Z. Ke, C. Yan, W. Ma, X. Zhan, *Chem. Mater.*, 2017, **30**, 239-245.
[24] F. Liu, Z. Zhou, C. Zhang, T. Vergote, H. Fan, F. Liu, X. Zhu, *J. Am. Chem. Soc.*, 2016, **138**, 15523-15526.
[25] S. j. Xu, Z. Zhou, W. Liu, Z. Zhang, F. Liu, H. Yan, X. Zhu, *Adv. Mater.*, 2017, **29**, 1704510.
[26] N. Qiu, H. Zhang, X. Wan, C. Li, X. Ke, H. Feng, B. Kan, H. Zhang, Q. Zhang, Y. Lu, Y. Chen, *Adv. Mater.*, 2017, **29**, 1604964.

[27] Y. Lin, Q. He, F. Zhao, L. Huo, J. Mai, X. Lu, C.-J. Su, T. Li, J. Wang, J. Zhu, Y. Sun, C. Wang, X. Zhan, *J. Am. Chem. Soc.*, 2016, **138**, 2973-2976.
[28] Y. Lin, F. Zhao, Q. He, L. Huo, Y. Wu, T. C. Parker, W. Ma, Y. Sun, C. Wang, D. Zhu, A. J. Heeger, S. R. Marder, X. Zhan, *J. Am. Chem. Soc.*, 2016, **138**, 4955-4961.
[29] S. Dai, F. Zhao, Q. Zhang, T.-K. Lau, T. Li, K. Liu, Q. Ling, C. Wang, X. Lu, W. You, X. Zhan, *J. Am. Chem. Soc.*, 2017, **139**, 1336-1343.
[30] D. Meng, H. Fu, C. Xiao, X. Meng, T. Winands, W. Ma, W. Wei, B. Fan, L. Huo, N. L. Doltsinis, Y. Li, Y. Sun, Z. Wang, *J. Am. Chem. Soc.*, 2016, **138**, 10184-10190.
[31] D. Meng, D. Sun, C. Zhong, T. Liu, B. Fan, L. Huo, Y. Li, W. Jiang, H. Choi, T. Kim, J. Y. Kim, Y. Sun, Z. Wang, A. J. Heeger, *J. Am. Chem. Soc.*, 2016, **138**, 375-380.
[32] Q. Wu, D. Zhao, J. Yang, V. Sharapov, Z. Cai, L. Li, N. Zhang, A. Neshchadin, W. Chen, L. Yu, *Chem. Mater.*, 2017, **29**, 1127-1133.
[33] J. Liu, S. Chen, D. Qian, B. Gautam, G. Yang, J. Zhao, J. Bergqvist, F. Zhang, W. Ma, H. Ade, O. Inganäs, K. Gundogdu, F. Gao, H. Yan, *Nat. Energy*, 2016, **1**, 16089.
[34] J. Zhang, Y. Li, J. Huang, H. Hu, G. Zhang, T. Ma, P. C. Y. Chow, H. Ade, D. Pan, H. Yan, *J. Am. Chem. Soc.*, 2017, **139**, 16092-16095.
[35] N. A. Ran, J. A. Love, C. J. Takacs, A. Sadhanala, J. K. Beavers, S. D. Collins, Y. Huang, M. Wang, R. H. Friend, G. C. Bazan, T.-Q. Nguyen, *Adv. Mater.*, 2015, **28**, 1482-1488.
[36] J. Zhang, L. Zhu, Z. Wei, *Small Methods*, 2017, **1**, 1700258.
[37] P. Cheng, M. Zhang, T.-K. Lau, Y. Wu, B. Jia, J. Wang, C. Yan, M. Qin, X. Lu, X. Zhan, *Adv. Mater.*, 2017, **29**, 1605216.
[38] Y. Zhang, X. Guo, B. Guo, W. Su, M. Zhang, Y. Li, *Adv. Func. Mater.*, 2017, **27**, 1603892.
[39] M. Zhang, X. Guo, W. Ma, H. Ade, J. Hou, *Adv. Mater.*, 2014, **26**, 5880-5885.
[40] N. A. Ran, S. Roland, J. A. Love, V. Savikhin, C. J. Takacs, Y.-T. Fu, H. Li, V. Coropceanu, X. Liu, J.-L. Brédas, G. C. Bazan, M. F. Toney, D. Neher, T.-Q. Nguyen, *Nat. Common.*, 2017, **8**, 79.
[41] J. Zhang, K. Jiang, G. Yang, T. Ma, J. Liu, Z. Li, J. Y. L. Lai, W. Ma, H. Yan, *Adv. Energy Mater.*, 2017, **7**, 1602119.
[42] H. Yao, Y. Li, H. Hu, P. C. Y. Chow, S. Chen, J. Zhao, Z. Li, J. H. Carpenter, J. Y. L. Lai, G. Yang, Y. Liu, H. Lin, H. Ade, H. Yan, *Adv. Energy Mater.*, 2018, **8**, 1701895.
[43] K. Vandewal, J. Benduhn, V. C. Nikolis, *Sustainable Energy & Fuels*, 2018, **2**, 538-544.
[44] I. Riedel, J. Parisi, V. Dyakonov, L. Lutsen, D. Vanderzande, J. C. Hummelen, *Adv. Func. Mater.*, 2004, **14**, 38-44.

A novel polymer P3TAE enables a high V_{OC} of 1.20 V and a PCE of 8.10% for non-fullerene OSCs.

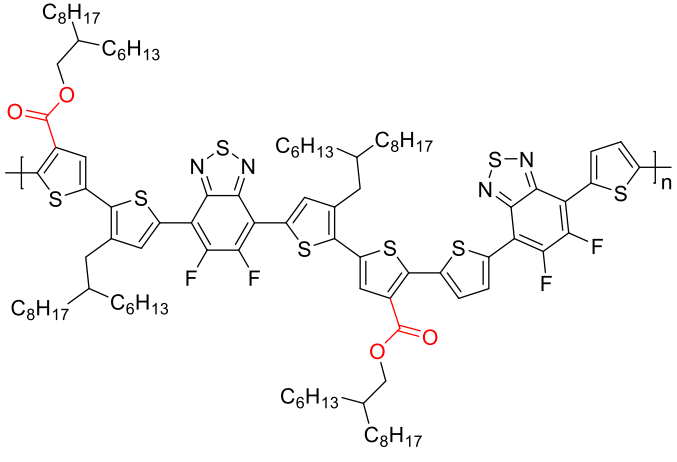

P3TAE